Development and metrological characterization of cement-based elements with self-sensing capabilities for structural health monitoring purposes

Gloria Cosoli[1], Alessandra Mobili[2], Elisa Blasi[2], Francesca Tittarelli[2,3], Milena Martarelli[1], Gian Marco Revel[1]

[1] *Dip. di Ingegneria Industriale e Scienze Matematiche, Università Politecnica delle Marche, Via Brecce Bianche snc - 60131 Ancona, Italy*
[2] *Dip. di Scienze e Ingegneria della Materia, dell'Ambiente ed Urbanistica, Università Politecnica delle Marche, Via Brecce Bianche snc - 60131 Ancona-INSTM Research Unit, Italy*
[3] *Istituto di Scienze dell'Atmosfera e del Clima, Consiglio Nazionale delle Ricerche, Via Gobetti 101 - 40129 Bologna, Italy*

ABSTRACT
Mortar specimens containing conductive additions (i.e., biochar and recycled carbon fibres – both alone and together, and graphene nanoplatelets) were characterized from a metrological point of view. Their piezoresistive capability was evaluated, exploiting the 4-electrode Wenner's method to measure electrical impedance in alternating current (AC); in this way, both material and electrode-material polarization issues were avoided. The selected mix-design was used to manufacture scaled concrete beams serving as demonstrators. Additionally, FEM-based models were realized for a preliminary analysis of the modal parameters that will be investigated through impact tests conducted after different loading tests, simulating potential seismic effects. The results show that the combined use of recycled carbon fibers and biochar provide the best performance in terms of piezoresistivity (with a sensitivity of 0.109 $(\mu m/m)^{-1}$ vs 0.003 $(\mu m/m)^{-1}$ of reference mortar). Conductive additions improve the Signal-to-Noise Ratio (SNR) and increase the material electrical conductivity, providing suitable tools to develop a distributed sensor network for Structural Health Monitoring (SHM). Such a monitoring system could be exploited to enhance the resilience of strategic structures and infrastructures towards natural hazards. A homogeneous distribution of conductive additions during casting is fundamental to enhance the measurement repeatability. In fact, both concrete intrinsic properties and curing effect (hydration phenomena, increasing electrical impedance) cause a high variability.

1. INTRODUCTION

The life cycle of cement-based structures can be optimized through proper measurements, in particular in the field of Structural Health monitoring (SHM). Indeed, the advantage of continuous monitoring is unquestionable with respect to periodic inspections, which can occur when it is already too late

to intervene effectively. Adequate interventions strategies can be adopted if measurement results timely highlight a potential damage in a structure/infrastructure [1]. Accordingly, it is possible to minimize management costs [2], which are higher as the time between damage occurrence and intervention increases (De Sitter's law [3]). In this way, the public administrations can prioritize the interventions on structures and infrastructures

identified through proper SHM technologies combined with an early warning system [4].

Sensors play a pivotal role in this field [5], especially if they have Internet of Things (IoT) capabilities that endorse data sharing, cloud services for computation (also with Artificial Intelligence – AI – technologies), and remote monitoring systems [6]. The best solution is probably represented by distributed sensor networks, able to gather data in many locations within the same structure, thus mapping the whole system and highlighting eventual criticalities in almost real-time [7]. Moreover, the collected data are exploited to constitute a dedicated database, which can be used to feed AI and Machine Learning (ML) algorithms for both prediction and classification purposes [8]–[10]. Furthermore, these data can be interfaced with the structure BIM (Building Information Model), hence keeping track of all the changes occurring over years [11]. Non-Destructive Techniques (NDTs) are among the most used systems for SHM, since they allow to measure significant parameters without taking samples to be analysed in laboratory. Standard sensors can be employed, such as accelerometers, load cells, inclinometers, GPS, environmental sensors, and also non-contact systems (e.g. laser-based sensors) [12]–[14]. The spatial resolution of the measurement results clearly depends on the sensors positioning; as mentioned above, distributed sensor networks are particularly relevant in this field, since they allow an actual mapping of the whole structure to be monitored, with a level of detail related to the final aims of the monitoring. In this context, also the cost of the hardware should be properly considered, being almost proportional to the nodes number. Even better results can be achieved combining monitoring and inspections procedures; the latter can be performed also with advanced techniques, such as sensorized drones (also known as Unmanned Aerial Vehicles, UAVs [15]). Amongst possible sensors, UAVs can have onboard environmental sensors for air quality assessment [16] or high-resolution multispectral vision-based systems to detect possible structural damages or degradation phenomena (e.g., caused by a prolonged exposure in an aggressive environment – such as chloride-rich solutions/aerosols). When inspection identifies an event of relevance, further tests can be planned, for example to assess the severity of the phenomenon (e.g., cracks aperture) [17], [18]. What is more, the scanning of a structure with a vision-based system embedded on a UAV allows to obtain a 3D model, showing the positioning and the severity of the identified defects or damages.

In recent years, SHM sensors are often coupled to self-sensing materials [19] (even better if eco-compatible and sustainable, as by-products or recycled materials). In this way, it is possible to develop distributed sensor networks with IoT capabilities, able to continuously gather data from remote buildings and infrastructures. This is particularly relevant in case of critical structures, which should be always operational, even after a catastrophic event, when the management of aftershock emergencies is pivotal. In this context, monitoring systems feeding early warning systems are very important to ensure public safety [13], [20]. Indeed, self-sensing materials confer many capabilities to the structure, easing its monitoring. Indeed, through self-sensing materials the structure perceives its own health status [21], being able not only to sense external loads (i.e., phenomena related to piezoresistive capacity), but also to detect the penetration of contaminants or identify defects and cracks. Many materials have been recently applied to pursue this aim, both in form of fibres and fillers. Among the others we can mention steel fibres [22], carbon fibres (both virgin and recycled), nickel powder [23], carbon nanotubes [24], graphene [25], graphite [26], foundry sand [27], carbon black [28], char, and biochar [29]. In a view of green and circular economy, recently particular interest has been shown on recycled material and by-products potentially having self-sensing capabilities; this strategy allows not only to reuse materials, but also to limit production costs. For example, in the European project EnDurCrete (New Environmental friendly and Durable conCrete, integrating industrial by-products and hybrid systems, for civil, industrial, and offshore applications, GA n° 760639, http://www.endurcrete.eu/) some of the present authors have developed self-sensing mix-designs for mortar and concrete including carbon-based additions, namely recycled carbon fibres and char or biochar. Also a patent (https://www.knowledge-share.eu/en/patent/eco-friendly-and-self-sensing-mortar/) has been granted on this invention, together with the related measurement system for electrical impedance ("Eco-compatible and self-sensing mortar and concrete compositions for manufacturing reinforced and non-reinforced constructive elements, related construction element and methods for the realization of self-monitorable building structures", patent n° 102020000022024). This can be exploited for SHM purposes in self-monitorable structures, whose life cycle will result optimised thanks to the continuous assessment of health status. The activities of EnDurCrete project are being followed up within the framework of the national project reCITY (Resilient City – Everyday Revolution, PON R&I 2014-2020, identification code: ARS01_00592, http://www.ponricerca.gov.it/media/396378/ars01_00592-decreto-concessione-prot369_10feb21.pdf), whose objective is to realize a multimodal monitoring system (modular and interoperable as much as possible) that can enhance the resilience of critical structures/infrastructures with respect to natural hazards, along with the resilience of energy distribution systems. Among natural threats, it is worth mentioning earthquakes and landslides (also interacting each other). Indeed, in Italy particular attention is paid to seismic risk, being Italy a seismic area, where important earthquakes often manifest in different regions, such as the crater of the centre of Italy. In the perspective of seismic protection of buildings and infrastructures, on the one hand, the strains caused by external loads should be assessed to analyse possible structural damages; on the other hand, the analysis of vibrations is pivotal to characterise the dynamic behaviour of the whole structure and identify possible criticalities. Lacanna et al. [30] considered a bell tower (Giotto's bell tower, Firenze, Italy) and studied its dynamic response through the combination of operational modal analysis and seismic interferometry. They evaluated frequency, shape modes, and seismic wave velocity, using a seismic sensor network capable to promptly identify eventual structural damages. The results showed that the analysed bell tower is a dispersive structure with bending deformation. Induced vibrations represent a great concern for concrete-based lifelines, such as bridges [31]: hence, control and mitigation of vibrations is fundamental. In the context of seismic monitoring, accelerometers are the most common sensors; just as an example, Oliveira et Alegre [32] applied accelerometers in the monitoring of dams. This way, they were able to describe natural frequencies, mode shapes, and seismic response over time. Indeed, in a seismic context SHM surely plays a pivotal role, even more when monitoring is sided by an early warning system based on the measured signals. In this way, the public administrations can be supported in decision-making strategies

definition, essential for risk management and for the prioritization of emergency interventions. In the reCITY project, the authors of this paper utilize data-fusion strategies together with Artificial Intelligence (AI) technologies to extract meaningful parameters related to the structural health status of a structure. This information can be exploited to set up an early warning system, promptly highlighting critical situations that should be timely considered, providing an efficient intervention. Furthermore, AI algorithms will be useful for prediction purposes as well, made possible through the ingestion of long-time series data for model training. Finally, the reCITY project aims to valorise good practices for resilience, supporting citizens community during emergency situations. To this aim, the data gathered through the monitoring system will be shared in dedicated platforms with user-friendly interfaces, thus allowing the creation of a formed, informed, trained, and active community, which is aware of the city status and has a proper sense of community.

This paper presents the results of the metrological characterization of different types of mortar with self-sensing capabilities, embedding sensing electrodes for electrical impedance measurement, thus proving their piezoresistive ability. The results were compared to standard measurements performed with traditional strain gages. Moreover, this work reports the first results on monitoring of demonstrative scaled prototypes realized with the best performing conductive additions in terms of self-sensing capability. In the near future, these prototypes will be subjected to loading tests and will be analysed in terms of dynamic response, hence demonstrating their potentiality for application within the monitoring platform, especially in a seismic context. Then, durability tests will be carried out and data will be acquired for a long time, thus collecting data useful for the training of AI algorithms in a view of early warning system. Indeed, this is pivotal to enhance the resilience of structures and infrastructures to natural hazards (like earthquakes).

The paper is organised as follows: the materials and methods are reported in Section 2, Section 3 shows the results, and the authors give their discussions and conclusions in Section 4, together with possible future developments.

2. MATERIALS AND METHODS

The main aim of the reCITY project is to develop a flexible and interoperable platform for the collection of multimodal signals and their sharing on a Cloud to deliver different services (e.g., data processing and AI algorithms exploitation for setting up early warnings and deriving significant indices for SHM purposes). The potentialities of this platform are relevant for managing emergencies and adopting adequate policies in the seismic context, thus improving the resilience of structures and infrastructures, especially when they are critical constructions.

Data from different sensors will be gathered from the project demonstrators, which will be described in the following sections. The pipeline related to the platform is reported in Figure 1.

The collected data will be stored both in a dedicated database and in FIWARE ecosystem (https://www.fiware.org/); FIWARE can deal with different types of data and can also merge new and existent data models, in a view of developing smart cities and systems capable to share information and knowledge with diverse stakeholders (e.g., institutions and public decision-makers, but also common citizens). In this way, the researchers' community can arise the awareness on the city structures and infrastructures, hence also improving the resilience towards possible emergency situations.

2.1. Metrological characterization of piezoresistive capacity

In a preliminary phase of the reCITY project, the authors considered mortar specimens to identify the best mix-design in terms of piezoresistive capacity. Different types of conductive additions were employed, and their behaviour was evaluated under laboratory conditions. These tests were performed to select the best performing carbon-based additions to be used for the casting of the project demonstrators (concrete beams), which will be further detailed. Indeed, those concrete specimens will be subjected to both loading tests and vibrational analyses, simulating the effect of a seismic event. The reCITY platform for SHM will include, among the others, electrical impedance sensors and accelerometers; in particular, the signals will be acquired through a low-cost system, the EVAL-AD5940 board (by Analog Device).

Within the context of piezoresistivity tests on mortar specimens, electrical impedance signals were compared with traditional strain gages deformation, to characterize these self-sensing materials in terms of metrological performance. For sure, this performance is affected by the conductive additions included in the mix-design.

Prismatic mortar specimens (40 mm × 40 mm × 160 mm, Figure 2) were realized according to 5 different mix-designs:

- Reference mortar specimens (REF), without conductive additions, to be considered as reference mixture;
- Biochar-based mortar (BCH). The by-product was provided by RES (Reliable Environmental Solutions) in pellet format, then was grinded and sieved at 75 μm before addition in mix-design (0.5 vol.%) in order to facilitate its distribution within the mixture;
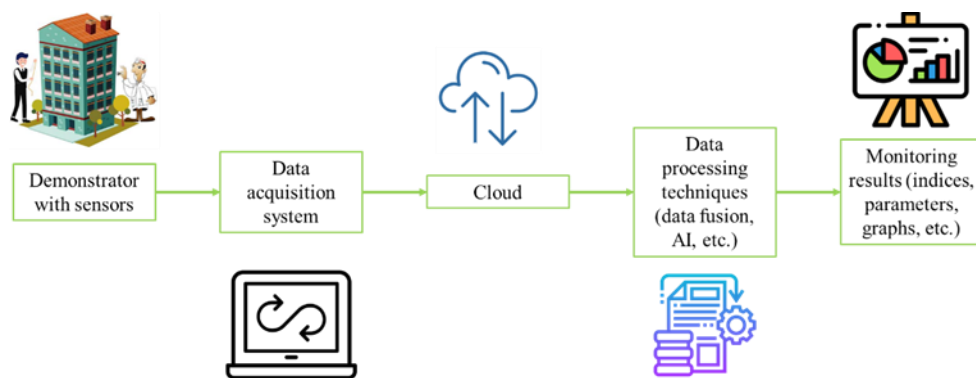

Figure 1. Scheme of data acquisition from demonstrators, sharing, processing and results.
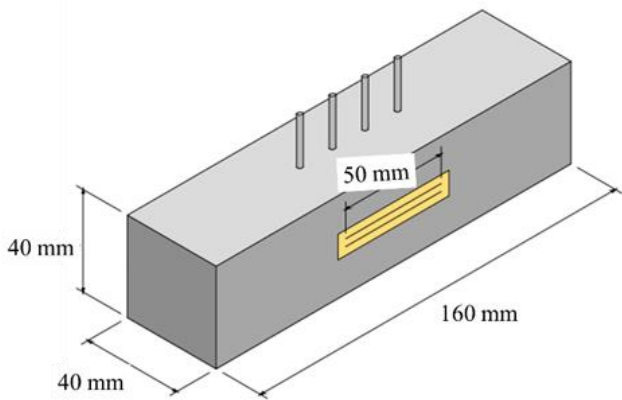
Figure 2. Geometry of the sensorized mortar specimen (strain gage and electrical impedance electrodes can be appreciated in the figure).

- Mortar containing 6-mm long recycled carbon fibres (RCF). The fibres were supplied by Procotex Belgium SA and were obtained mixing carbon fibres of different origins and graphite from pure carbon fibres coils. A mean average density of 1.85 g/cm³ was considered and the fibres were added in 0.05 vol.%;
- Mortar with both biochar and recycled carbon fibres (BCH+RCF), at the same dosages used in BCH and RCF specimens (i.e., 0.5 vol.% and 0.05 vol.%, respectively);
- Mortar manufactured with graphene nanoplatelets (GNP), having a thickness of 6-8 nm and a size lower than 5 μm, in 0.5 vol.%. In particular, Pentagraf 30 graphene nanoplatelets (produced by Pentachem S.r.l.) were used; their specific surface area (measured with BET adsorbance method, Brunauer, Emmett, Teller) was equal to 30 m²/g.

To manufacture mortar specimens, we used Portland cement (CEM II/A-LL) and a calcareous sand (0-8 mm) as fine aggregate, mixing it with 5.5 wt.% water to reach saturated surface dried (s.s.d.) conditions. The water/cement ratio (w/c) was the same for all the mortar specimens and was equal to 0.55 by mass, whereas the aggregate/cement ratio (a/c) was equal to 3 by mass. The mortars workability (x, measured according to UNI EN 1015-3 standard) was equal to 140 mm $\leq x \leq$ 200 mm (i.e., plastic workability).

The mix-designs referred to each type of mortar are reported in Table 1.

To characterize the mortars in terms of piezoresistive capacity, electrical impedance measurements should be carried out. Hence, 4 stainless steel rods (diameter: 3 mm; length: 40 mm; inter-electrode distance: 12 mm), acting as electrodes, were embedded (half length) in the specimens centreline, in order to exploit the Wenner's configuration method [33] in alternating current (AC, in particular with a measurement frequency higher than 1 kHz), hence avoiding both electrode-interface and
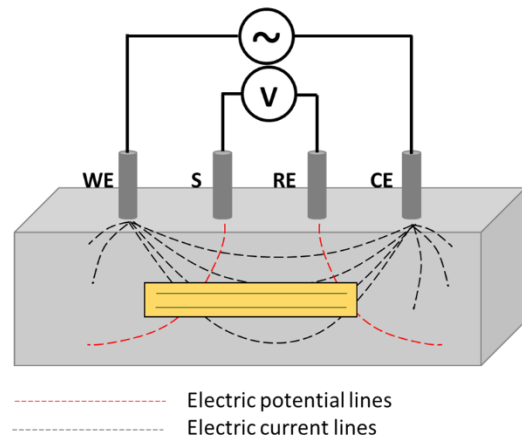

Figure 3. Wenner's method applied on a mortar specimen: electric current is applied between the external electrodes (i.e. WE and CE) and the corresponding electric potential drop is measured between the internal ones (i.e. S and RE).

material polarization effects, which would affect the measurement result with a significant uncertainty value.

After the casting phase, specimens were cured in a temperature (T) and relative humidity (RH) controlled environment (T = (20 ± 1) °C; RH = (95 ± 5) %) for 7 days, being wrapped by plastic sheets. Then, they were left at T = (20 ± 1) °C and RH = (50 ± 5) % without any cover. During the curing phase, the mortar specimens were regularly monitored in terms of both mechanical resistance and electrical impedance, with measurement carried out at 2, 7, and 28 days. Compressive strength was assessed with a hydraulic press (Galdabini, with an applicable maximum load of 200 kN), considering the average value obtained on 3 dedicated specimens of the same type. On the other hand, electrical impedance was assessed through electrical impedance spectroscopy method, employing a potentiostat/galvanostat (Metrohm) with a 4-electrode configuration (Figure 3), on the prismatic mortar specimens with electrodes.

The loading tests were performed after the completion of curing phase. A mechanical press (Zwick Roell Z050) was employed to apply a maximum load equal to 11.5 kN. The value of the applied load was set in order to remain in the elastic range of the material [34], which was measured on the REF mortar during curing; in particular, 20% of the obtained compressive strength of the REF specimen was chosen. Hence, the formation of cracks was avoided, as well as the alteration of the specimen mechanical properties. Each specimen was subjected to 5 loading cycles per test and the test was repeated three times in different weeks (in a time interval of 8 weeks), for a total of 15 loading cycles per specimen. With this test protocol, also the variability due to hydration phenomena plays a relevant role on the measured electrical impedance.

The complete test setup is reported in Figure 4, where it is possible to observe the ZwickRoell mechanical press, equipped with a load cell (full scale: 50 kN), used to load the mortar specimen, on which a strain gage specific for cement-based materials (HBK, net grid length: 50 mm) was installed. Spider8 system by HBM was employed to acquire strain gages signals, adopting a half-bridge configuration to compensate eventual external disturbs. Moreover, a preliminary test was performed to compare the results obtained with half- and full-bridge configurations. To this aim, a BCH specimen was subjected to 5

Table 1. Mortars mix-design (kg/m³).

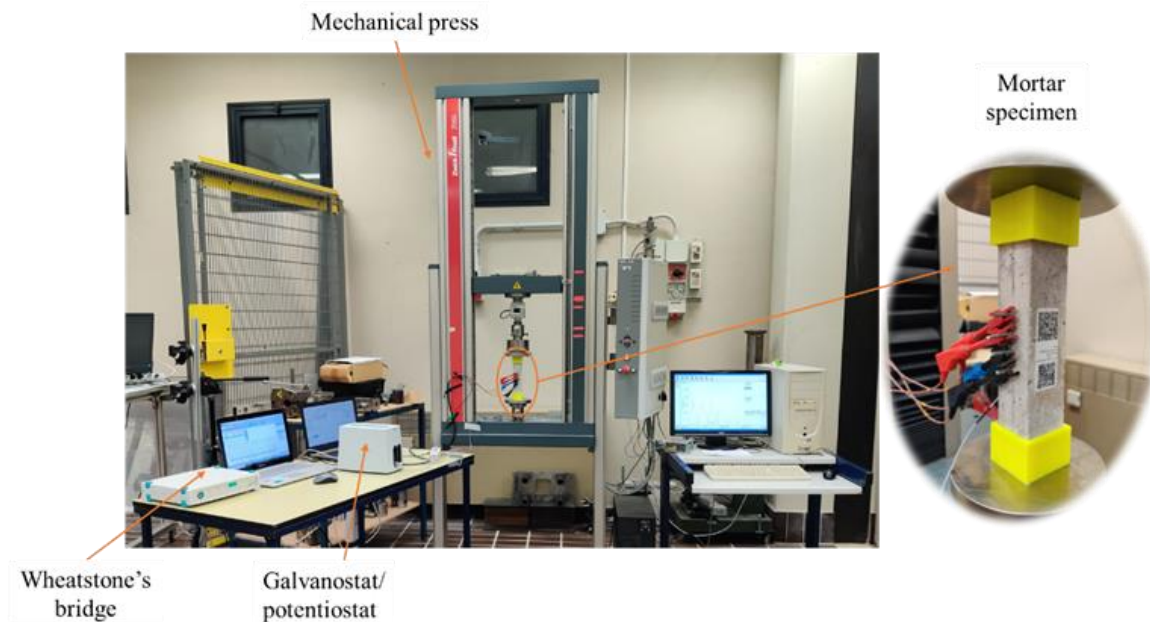| Mix	Cement	Water	Sand	RCF	BCH	GNP
REF	499	274	1497	-	-	-
RCF	499	274	1496	1	-	-
BCH	496	273	1489	-	10	-
BCH+RCF	496	273	1488	1	10	-
GNP	496	273	1489	-	-	10

Figure 4. Measurement setup for piezoresistivity tests: loads are applied on the tested mortar specimen through a mechanical press; hence, strain and electrical impedance are measured by means of a Wheatstone's bridge and a galvanostat/potentiostat, respectively.

repeated loading cycles and the strain was assessed with both the Wheatstone's bridge configurations.

Data analysis focused on the real part of electrical impedance, which in literature is the most associated one to the structural conditions of the material [35].

2.2. Design and realization of the project demonstrators

To verify the behaviour of self-sensing materials in a seismic context, the authors designed loading tests and vibrational analyses on scaled demonstrators. In particular, 1:5 scaled reinforced concrete beams (10 cm × 10 cm × 50 cm) were planned in detail, both in terms of materials and embedded sensors. For the former, the best conductive additions and dosages resulting from piezoresistivity tests were chosen; for the latter, different types of sensors were selected, namely:

- Electrical impedance sensors, which are fundamental to show the piezoresistive capacity of the concrete elements;
- Accelerometers, mounted on specific bases fixed on the upper specimen surface to measure the dynamic response of the structure to external excitation (provided with an impact hammer, as it will be described in detail);
- Sensors for the monitoring of rebar free corrosion potential, useful to early detect the concrete deterioration as cracking or water penetration occur [38] (CoSMoNet - Concrete Structures Monitoring Network, Università Politecnica delle Marche, Patent n° 0001364988). Indeed, after loading and vibrational tests, the specimens will be subjected to accelerated degradation tests; hence, the presence of cracks generated during loading could ease the penetration of contaminants into the material.

The geometry of the prototype is reported in Figure 5; 20 degrees of freedom for the measurement of the specimen dynamic response are foreseen (stainless-steel washers are positioned on the specimen upper surface through bicomponent acrylic resin, in order to easily install the accelerometers during experimental modal analysis through beeswax), whereas the

excitation point is set on the specimen centreline. The specimen has a reinforcing steel rebar at its centre, where different sensors are placed:

- Electrode arrays for electrical impedance measurement;
- Pseudo-reference electrode for the measurement of the rebar free corrosion potential (CoSMoNeT sensor [36]).

The impact test will be carried out with a sensorized impact hammer (PCB 086 B04), equipped with a load cell for the measurement of the provided force. In this way, possible effects of earthquake are simulated, including cracking phenomena linked to external forces acting on the structural element. Hence, the dynamic response is evaluated at time 0 (as-is conditions) and after each applied load, to observe possible modifications in the modal parameters of the element.
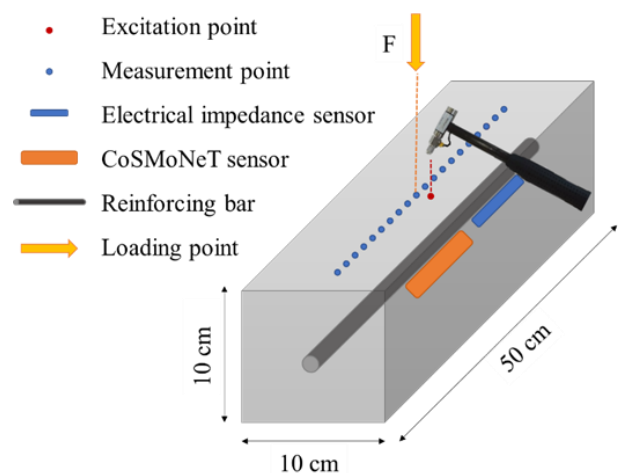

Figure 5. Geometry of the demonstrator prototype with sensors, namely electrode array for electrical impedance measurement, electrode for the measurement of the rebar free corrosion potential (i.e. CoSMoNeT sensor), as well as excitation and acceleration measurement points for impact test.

2.2.1. Manufacturing of concrete demonstrators

No. 9 concrete specimens were manufactured as follows:

- 3 sensorized concrete beams, to be subjected to loading tests and vibrational analyses;
- 3 sensorized concrete beams, to maintain undamaged (i.e., reference specimens);
- 3 non-sensorized concrete beams, to be subjected to loading tests and vibrational analyses. These serve to evaluate the effect of the embedded sensors, representing discontinuities for the material.

To manufacture concrete specimens, we used Portland cement (CEM II/A-LL) and a calcareous sand (0-4 mm) as fine aggregate, whereas intermediate (5-10 mm) and coarse (10-15 mm) river gravels were used as coarse aggregates. RCF and BCH were added at 0.5 vol.% and 0.05 vol.% on the total, respectively, as conductive additions (being them resulted the best performing additions in terms of piezoresistive capability, see Section 3.1.2). The w/c ratio was set at 0.50 by mass to reach the S5 workability class. The mix-design is reported in Table 2.

The casting phase was carried out using a concrete mixer; at first, the solid components were mixed together for 8 minutes, then water was added and mixed for additional 10 minutes. To manufacture sensorized/non-sensorized reinforced specimens, the fresh mix was poured in prismatic moulds (10 cm × 10 cm × 50 cm); in addition, cubic specimens (side: 10 cm) were realized for compressive strength tests (performed at 1, 7, and 28 days according to the EN 12390-3 standard). Moreover, also flexural strength was assessed on dedicated 10 cm × 10 cm × 50 cm non-sensorized reinforced specimens, according to the EN 12390-5.

2.2.2. FEM numerical model

In order to carry out a preliminary test in terms of modal analysis, numerical simulations were made in COMSOL Multiphysics® environment, exploiting Finite Element Method (FEM). In particular, the designed concrete beam was simulated in different configurations:

- Scaled (10 cm × 10 cm × 50 cm) and life-size (50 cm × 50 cm × 250 cm) concrete specimens, without reinforcing rebar;
- Scaled (10 cm × 10 cm × 50 cm) concrete specimen, with reinforcing rebar;
- Scaled (10 cm × 10 cm × 50 cm) concrete specimen, with reinforcing rebar and embedded sensors.

Table 2. Concrete mix-design (kg/m³).

Cement	470
Water	235
Air (%)	2.5
Sand	795
Intermediate gravel	321
Coarse gravel	476
RCF	1
BCH	10

Indeed, the embedded sensors represent discontinuities inside the specimen; analogously, the plastic tubes used for installing the reinforcement rebar and the sensors influence the modal parameters of the structural element. Hence, these preliminary models help to better understand the behaviour of the element in loading and vibrational tests, as well as to identify the natural frequencies of interest and the related modal shapes in both sensorized and non-sensorized beams.

The geometry of the sensorized and non-sensorized reinforced concrete models is reported in Figure 6 and in Figure 7, respectively.

3. RESULTS

This section reports the results related to the different research activities described in this paper, namely:

- The results related to mortar specimens (Section 3.1), including the monitoring of mechanical strength and electrical impedance of the different mix-design mortar specimens during curing (Sub-section 3.1.1) and the results from piezoresistivity tests, together with the results of preliminary comparison tests between half-bridge and full-bridge configurations (Sub-section 3.1.2);
- The preliminary results related to the concrete beam demonstrators (Section 3.2) in terms of mechanical strength characterization (Sub-section 3.2.1), the monitoring of electrical impedance during curing (Sub-section 3.2.2), and the mode shapes resulting from FEM-based numerical simulations on both sensorized and non-sensorized concrete specimens (Sub-section 3.2.3).
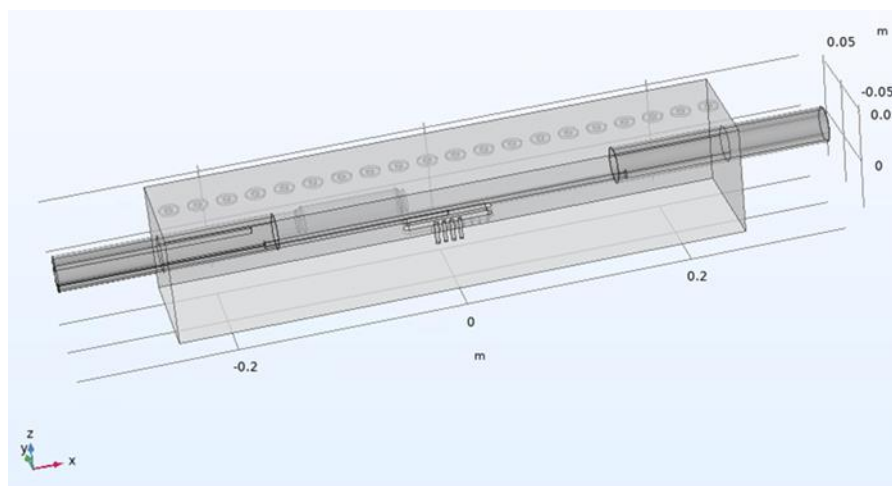

Figure 6. Geometry of the FEM model related to the scaled sensorized concrete specimen.
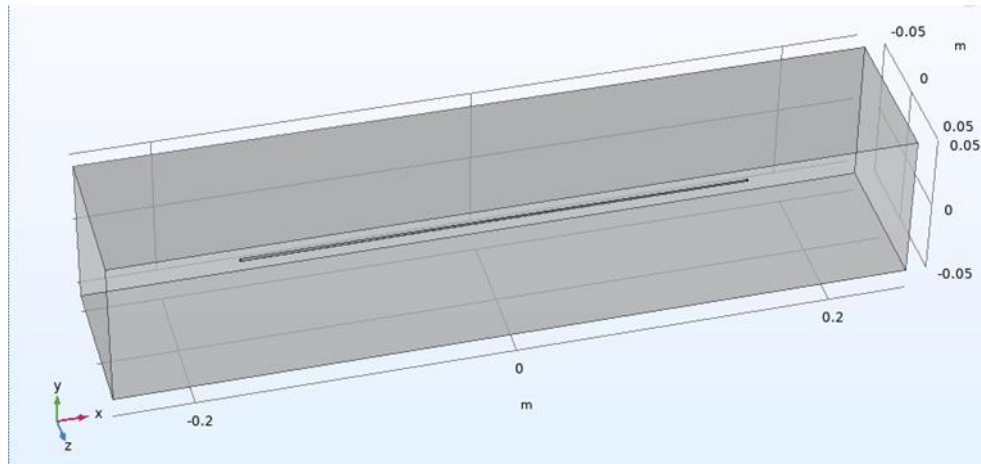
Figure 7. Geometry of the FEM model related to the scaled non-sensorized concrete specimen.

3.1. Monitoring and piezoresistivity tests on mortar specimens

In this section, the results related to the monitoring during curing phase of mortar specimens (in terms of both mechanical strength and electrical impedance) and the piezoresistivity tests, together with the comparison between half-bridge and full-bridge configurations for the strain measurement, are reported.

3.1.1. Monitoring during curing phase

The results in terms of compressive strength and real part of electrical impedance are reported in Figure 8 and Figure 9, respectively. It is possible to observe an increase in both values, as expected during curing, since hydration of the material is occurring, hence electrical impedance and mechanical strength increase [37]. Furthermore, mechanical strength at 28 days is enhanced through the addition of RCF to the mortar mix-design, passing from 36 MPa (REF specimen) to 40 MPa and 43 MPa for BCH+RCF and RCF specimens, respectively. Thus, it can be stated that the addition of RCF improves the mechanical performance of the material, thanks to the presence of carbon micro-particles on their surface acting as nucleation points for the formation of C–S–H crystals [38], [39]. Also the self-sensing properties should be enhanced, given that RCF contribute to decrease the material electrical resistivity; in particular, a decrease of 85 % and 92 % is obtained for RCF and BCH+RCF mixtures, respectively. In this way, it is possible to exploit relatively low-cost sensors for the monitoring of electrical impedance, hence enabling the realization of multiple modes sensor networks for SHM purposes [2]. Observing Figure 9, it is possible to notice

relevant differences in terms of electrical impedance among diverse mix-designs. This was expected and is attributable to the different conductive additions employed to realize the mortar specimens. Indeed, RCF significantly decrease the electrical resistivity of the final material, thanks to their good electrical conductivity properties.

3.1.2. Piezoresistivity tests

Preliminary tests were carried out to compare the results obtainable with a half-bridge and a full-bridge configuration for the measurement of strain of a mortar specimen (namely a BCH specimen) subjected to cyclic loading tests. The results provided a repeatability range of 18 $\mu\varepsilon$ and 4 $\mu\varepsilon$ for half-bridge and full-bridge configurations, respectively; moreover, a repeatability deviation of 7 $\mu\varepsilon$ and 2 $\mu\varepsilon$ was obtained in the two cases, respectively. Given that these values are acceptable for the in-field application of interest, the half-bridge configuration was selected for the rest of piezoresistivity tests. Indeed, it is an optimal compromise between metrological performance (accuracy and sensitivity – gage factor) and ease of installation as well as cost (also in view of distributed sensor networks realization).

The results of the piezoresistivity tests are reported in Table 3; in particular, the mean (μ) and standard deviation (σ) values are reported for applied maximum loading force (F_{max}), maximum strain (ε_{max}), variation of the real part of electrical impedance (ΔZ_{Re}) and related electrical impedance at 0-time (Z_{Re_t0}), and sensitivity of electrical impedance real part towards strain. Results are reported for all the tested mix-designs and are
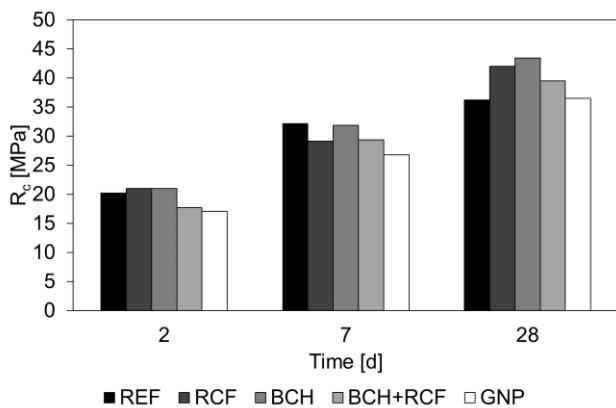

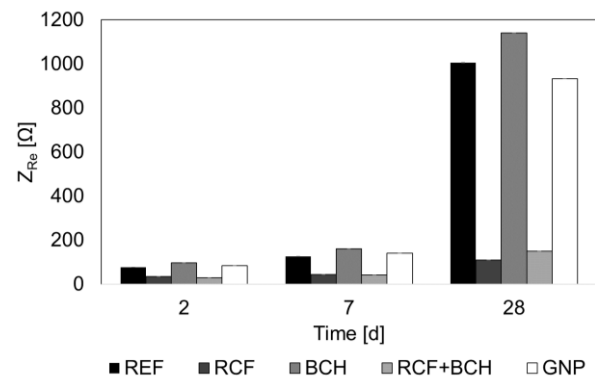Figure 8. Mechanical strength of mortar specimens during curing phase.

Figure 9. Real part of electrical impedance of mortar specimens during curing phase.

Table 3. Results obtained for the different mix-designs (reported as mean (standard deviation)).

Mix-design	F_{max} in N	ε_{max} in µm/m	ΔZ_{Re} in Ω	Z_{Re_t0} in Ω	Sensitivity in (µm/m)$^{-1}$
REF	11516.20 (6.25)	157 (73)	23.16 (18.25)	5673.10 (3572.57)	0.003 (0.002)
RCF	11512.16 (2.05)	181 (78)	0.92 (0.33)	203.14 (24.71)	0.004 (0.003)
BCH	11511.57 (2.11)	217 (119)	22.25 (15.30)	5725.73 (6071.60)	0.008 (0.009)
BCH+RCF	11512.76 (1.26)	155 (49)	70.26 (26.46)	419.07 (71.15)	**0.109** (0.026)
GNP	11511.88 (2.04)	226 (88)	9.86 (8.08)	6605.27 (4999.12)	0.001 (0.000)

averaged on the 15 loading cycles applied on each specimen. As expected, quite high values of standard deviation were obtained for electrical impedance. They can be attributed to the ageing process of the specimens (causing the material hydration – tests were performed in a time span of 8 weeks), which on the other hand cause also significant variations in terms of mechanical elasticity, reflecting into high standard deviation values for strain parameter. The sensitivity of electrical impedance towards strain (and, hence, external load) is improved by conductive additions. Sensitivity passes from 0.003 µε^{-1} for REF mortar specimen to 0.109 µε^{-1} for BCH+RCF one; in this case, in fact, the lower electrical resistivity leads to a higher percentage variation of electrical impedance. For the sake of completeness, it should be noted that RCF alone do not provide the same performance to mortar, at least at the considered load values; for this reason, biochar plays a key role in the provision of piezoresistive properties. Moreover, high variability is observed also in the response of self-sensing materials in terms of electrical impedance variations; for example, considering BCH+RCF mortar, a standard deviation of 26.46 Ω for a mean value of 70.26 Ω is reported for ΔZ_{Re} quantity. This fact could be due to both hydration phenomena occurring over time (thus changing the material morphology and composition), as well as to the fact that cement-based materials (e.g., mortar and concrete) are inhomogeneous by definition. For this reason, significant variability could be observed also among specimens manufactured according to the same mix-design.

In any case, the variations of the real part of electrical impedance mirror quite well the applied load and, hence, the strain of the specimen. An example of this behaviour is reported in Figure 10 for BCH+RCF specimen (5 loading cycles are considered); in particular, it is possible to observe that Z_{Re} decreases with increasing applied load, since compression causes a decrease of the specimen length and, hence, of the sensing
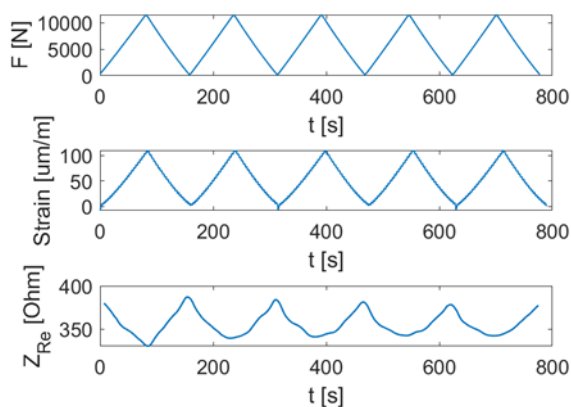
volume interested by the sensing electrodes. However, a low-moderate strength of linear correlation was evidenced for all the tested mortar specimens, with the exception of BCH+RCF mortar, where the Pearson's correlation coefficient was equal to 0.8 (Figure 11).

3.2. The concrete beam project demonstrators

In this section preliminary results related to the manufactured concrete beams as reCITY project demonstrators (Figure 12) are reported.

3.2.1. Mechanical strength

The compressive strength measured on dedicated specimens is reported in Figure 14. As expected, the compressive strength increases over time, reaching an average value of 40 MPa at 28 days, with a standard deviation of 1 MPa. Concerning the flexural strength, an average value of 14 MPa was obtained, with a standard deviation of 1 MPa.

3.2.2. Monitoring of electrical impedance during curing

The electrical impedance data (in particular, in terms of real part, Z_{Re}) is reported in Figure 15. As expected, Z_{Re} increases over time while only a specimen (i.e., C) is quite different from the others; this may be due to some particularly big aggregates present within the sensing volume.

3.2.3. FEM numerical model

The results obtained from scaled and life-size non-reinforced beams show that the natural frequencies vary together with the scaling factor; in particular, the natural frequencies will be 5 times those of the life-size element. For example, considering the first mode shape (Figure 13), the natural frequency is estimated at 241 Hz for the life-size structure ($f_{n,real}$) and at 1205 Hz for the scaled beam ($f_{n,scaled}$); this means that $f_{n,scaled}$ is approximately 5 times $f_{n,real}$. For this reason, it is necessary to evaluate the effects of a seismic event at frequencies higher than those typical of an
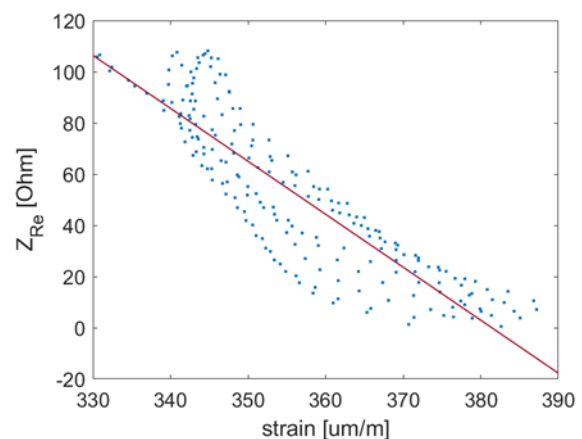

Figure 10. Results in terms of loading force (F, top), strain (ε, centre), and real part of electrical impedance (Z_{Re}, bottom) – example for BCH+RCF mortar specimen.

Figure 11. Evaluation of the linear correlation between the real part of electrical impedance (Z_{Re}) and strain – the red line is the interpolating line (RCF+BCH mortar specimen).
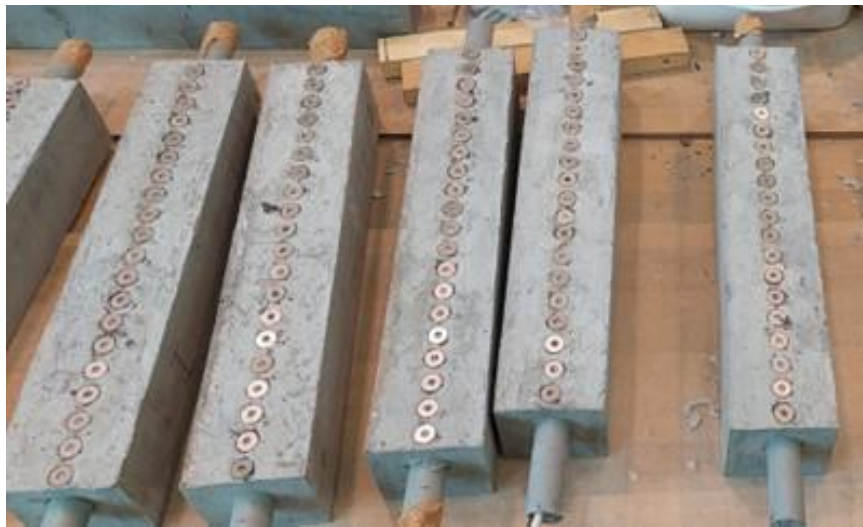
Figure 12. Example of the manufactured concrete beam demonstrators; tubes for installing the steel rebars and sensors are visible at the specimen extremities, whereas stainless-steel washers for the installation of accelerometers for modal analysis can be observed on the specimens top face.

earthquake, which are in the range of 1-10 Hz [40], [41]. The reinforcing rebar seems to not influence the natural frequencies of the concrete beam, at least at frequencies up to 4000 Hz, which will be the spectral range considered in the experimental modal analysis; this means that the geometry of the rebar is not particularly influencing in terms of the element rigidity. However, the presence of the external tubes modifies the *dynamic behaviour of the structural element; in particular, the* nodal lines of the

first mode shape (Figure 16) move on the tubes themselves and the related natural frequency increases up to 1529 Hz (approximately + 27 %). This means that the structural element is slightly stiffer because of the embedded components, which also influence the deformation, as well as making the specimen less homogeneous.

Considering the second mode shape, it is possible to observe that the presence of plastic tubes introduces two additional nodal lines located on the tubes themselves, even if the associated natural frequency is almost the same (i.e., 2841 Hz for the non-sensorized specimen, Figure 17, against 2846 Hz for the sensorized one, Figure 18).
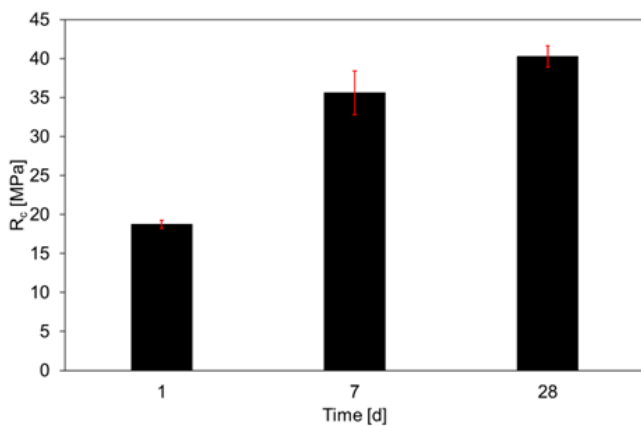
4. DISCUSSION AND CONCLUSIONS

This paper introduced the monitoring platform being developed in the framework of the reCITY project (identification code: ARS01_00592); in particular, the resilience of cement-based structures against seismic events are considered in the presented research activities. At first, the authors investigate different mix-designs of mortar in terms of piezoresistive capability; hence, sensorized concrete beams are designed and realized with the better mix-design to serve as the project demonstrators. Preliminary FEM numerical models are realized to analyse the modal parameters of the structural elements and the effect of the discontinuities represented by the embedded sensors.

Figure 14. Compressive strength of concrete specimens during curing phase.
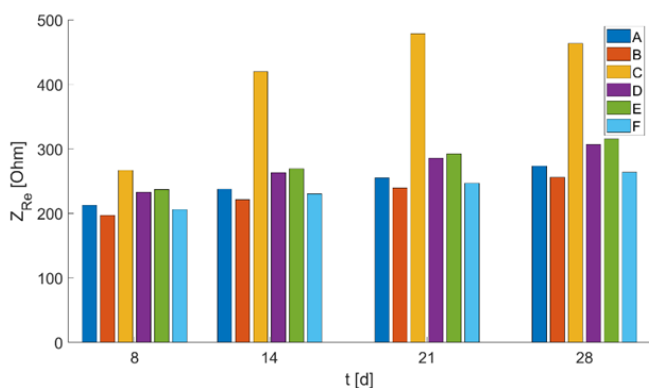

Figure 15. Real part of electrical impedance measured during curing on the 6 sensorized specimens.
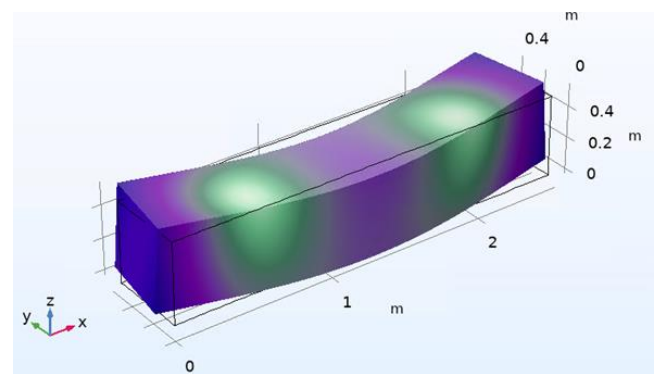

Figure 13. First mode shape for life-size beam (natural frequency: 241 Hz, corresponding to 1205 Hz for the 1:5 scaled beam).
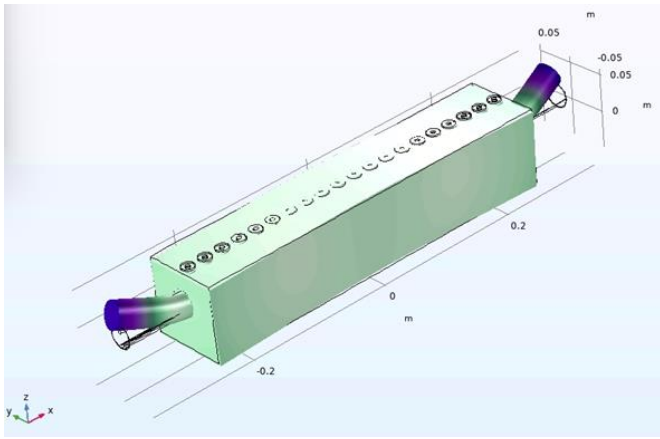
Figure 16. First mode shape for scaled sensorized beam (natural frequency: 1529 Hz).

The results show that carbon-based conductive additions in form of filler and fibres (namely biochar, BCH, and recycled carbon fibres, RCF) allow to obtain the best performance in terms of sensitivity to external loads. In particular, the measured electrical impedance shows a trend mirroring the one of the applied loads and, consequently, of the strain induced to the specimen. In this way, an electrical quantity (electrical impedance) reflects the behaviour of a mechanical quantity (strain), hence a sensor with self-sensing capacities is obtained. The metrological characterization of the phenomenon is pivotal and evidences the key role played by the type of conductive materials added to the mix-design. In fact, conductive additions have a twofold role: on the one hand, they decrease the material electrical resistivity, thus improving the circulation of electric current and easing the electrical impedance measurement; on the other hand, they improve the quality of the electric signal, decreasing the noise effect and, thus, enhancing the Signal-to-Noise Ratio (SNR). The best performance in terms of piezoresistive capability was obtained by the mix-design containing both BCH and RCF, resulting in the highest sensitivity towards strain; in particular, the average sensitivity of BCH+RCF mortar was equal to 0.109 $(\mu m/m)^{-1}$, against 0.003 $(\mu m/m)^{-1}$ of REF specimen. For this reason, these types and dosages of conductive additions were chosen for the realization of concrete scaled beams to serve as demonstrators of the reCITY project. Furthermore, the selected conductive additions are green sustainable by-products, so they can be fruitfully exploited also in a view of an environmentally friendly circular economy.
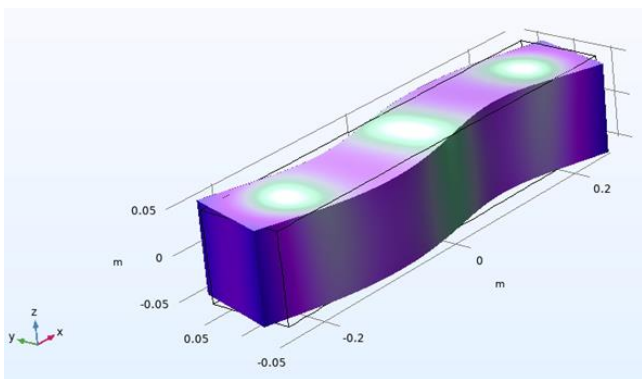
It is worthy to underline that a homogeneous distribution of conductive additions is fundamental. Indeed, cement-based materials are inhomogeneous by definition; hence, the distribution of components during casting phase is pivotal. Moreover, the electrical impedance measurement is local and is related to a limited sensing volume (depending on the inter-electrode spacing chosen according to the Wenner's method, in the 4-electrode AC configuration). Thus, it would be fundamental to optimize the manufacturing procedure to enhance the metrological performance of sensors based on self-sensing materials, especially in terms of measurement repeatability. Furthermore, it should be considered also the fact that electrical impedance depends not only on the external loads, but also on several different variables, such as environmental parameters (temperature and relative humidity), damages and cracks, penetration of contaminants, carbonation phenomena, etc. For this reason, electrical impedance should be analysed not in absolute values, but in terms of trend variations, so as to be able to detect unexpected peaks or variations (differing from the normal daily changes [2]) that require ad hoc investigations (e.g. specific inspections).

Electrical impedance measurements can provide a lot of information on the structure health status and boundary conditions, resulting particularly suitable for data fusion techniques used in a view of extracting meaningful indicators in the context of SHM. The sensing electrodes used for electrical impedance assessment could somehow substitute the traditional strain gages, which are much more expensive and difficult to install, besides being more delicate and requiring a more sophisticated acquisition circuit (i.e., Wheatstone's bridge).

In the future, the realized concrete specimens will be subjected to loading tests with increasing load values (starting from 50% of the concrete flexural strength until failure load), in order to progressively drive cracking phenomena. Modal analysis will be performed on the specimen as-is (time 0) and just after the execution of each load test. In this way, it will be possible to evaluate the effects of external loads and cracks on the modal parameters of the element, representing its "footprint". Both variations of natural frequencies and changes in the mode shape or mode curvature will be analysed, with the objective to both detect cracking onset and assess the severity of the damage. Moreover, vision-based techniques will be exploited for the detection and the quantitative assessment of cracking phenomena; an automated measurement system developed within the framework of the EnDurCrete European project will be exploited to this aim. Moreover, after the execution of loading

Figure 17. Second mode shape for scaled non-sensorized beam (natural frequency: 2841 Hz).
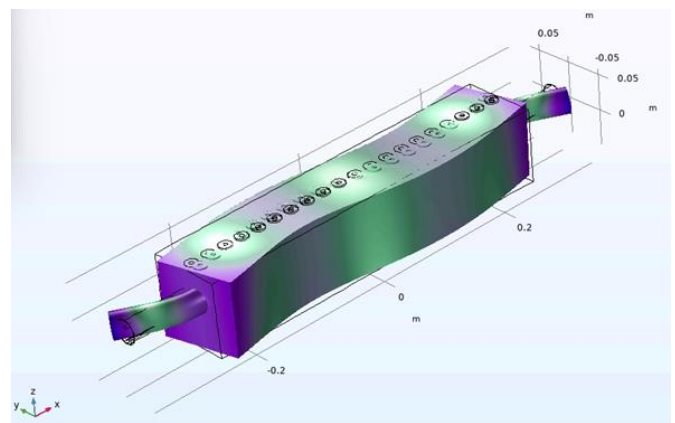

Figure 18. Second mode shape for scaled sensorized beam (natural frequency: 2846 Hz).

tests and related experimental modal analysis, all the concrete specimens will be subjected to accelerated durability tests, in particular to the exposure in water solutions. The aim is to evaluate how damages caused by seismic events can impact on the material durability.

In the reCITY project the electrical impedance data will be combined to the signals measured by means of standard transducers; they will be exploited also together with modal parameters coming from vibrational analyses, thus contributing to characterize a cement-based structure from a broader perspective. In fact, the multidomain information, properly analysed through AI-bases algorithms, can support decision-making processes and management procedures regarding critical structures. This allows to prioritize the interventions needed to guarantee the community safety and wellbeing, also enhancing the resilience towards natural hazards and emergency situations. Moreover, the reCITY platform will enable data sharing, so as to arise the community awareness on these aspects, making a society not only informed but also formed and active in the management of the (smart) city structures in an environment that inevitably becomes more and more urbanized.

ACRONYMS

AC	Alternating Current
AI	Artificial Intelligence
BCH	Biochar
BIM	Building Information Model
FEM	Finite Element Model
GNP	Graphene NanoPlatelets
ML	Machine Learning
NDT	Non-Destructive Technique
RCF	Recycled Carbon Fibers
RH	Relative Humidity
SHM	Structural Health Monitoring
SHR	Signal-to-Noise Ratio
SSD	Saturated Surface Dried
UAV	Unmanned Aerial Vehicle
W/C	Water-to-Cement ratio

ACKNOWLEDGEMENT

REFERENCES

[1] Dipartimento della Protezione Civile, Indicazioni operative per il raccordo e il coordinamento delle attività di sopralluogo tecnico speditivo, Italy, 2018, p. 29. Online [Accessed 22 June 2023] [In Italian]
https://www.lazio.beniculturali.it/wp-content/uploads/2021/03/DPC-Indicazioni-operative.pdf

[2] N. Giulietti, P. Chiariotti, G. Cosoli, G. Giacometti, L. Violini, A. Mobili, G. Pandarese, F. Tittarelli, G. M. Revel, Continuous monitoring of the health status of cement-based structures: electrical impedance measurements and remote monitoring solutions, Acta IMEKO, vol. 10, no. 4, Dec. 2021, pp. 132–139.
DOI: 10.21014/ACTA_IMEKO.V10I4.1140

[3] W. R. de Sitter, Costs of service life optimization 'The Law of Fives', Comité Euro-International du Béton, 1984, pp. 131–134.

[4] M. P. Limongelli, Monitoraggio strutturale per la protezione sismica del patrimonio edilizio, Tra Prev. e cura la Prot. del Patrim. Edil. dal rischio Sism., 2013, pp. 36–48. [In Italian]

[5] S. Das, P. Saha, A review of some advanced sensors used for health diagnosis of civil engineering structures, Measurement, vol. 129, Dec. 2018, pp. 68–90.
DOI: 10.1016/J.MEASUREMENT.2018.07.008

[6] F. Lamonaca, C. Scuro, P. F. Sciammarella, R. S. Olivito, D. Grimaldi, and D. L. Carnì, A layered IoT-based architecture for a distributed structural health monitoring system System, Acta IMEKO, vol. 8, no. 2, Jun. 2019, pp. 45–52.
DOI: 10.21014/acta_imeko.v8i2.640

[7] C. Scuro, D. L. Carnì, F. Lamonaca, R. S. Olivito, G. Milani, Preliminary study of an ancient earthquake-proof construction technique monitoring by an innovative structural health monitoring system, Acta IMEKO, vol. 10, no. 1, Mar. 2021, pp. 47–56.
DOI: 10.21014/acta_imeko.v10i1.819

[8] W. Dong, Y. Huang, B. Lehane, G. Ma, An artificial intelligence-based conductivity prediction and feature analysis of carbon fiber reinforced cementitious composite for non-destructive structural health monitoring, Eng. Struct., vol. 266, Sep. 2022, p. 114578.
DOI: 10.1016/J.ENGSTRUCT.2022.114578

[9] S. Meisenbacher, M. Turowski, K. Phipps, M. Rätz, D. Müller, V. Hagenmeyer, R. Mikut, Review of automated time series forecasting pipelines, Wiley Interdiscip. Rev. Data Min. Knowl. Discov., Feb. 2022.
DOI: 10.1002/widm.1475

[10] Sh. K. Baduge, S. Thilakarathna, J. Sh. Perera, M. Arashpour, P. Sharafi, B. Teodosio, A. Shringi, P. Mendis, Artificial intelligence and smart vision for building and construction 4.0: Machine and deep learning methods and applications, Autom. Constr., vol. 141, Sep. 2022, p. 104440.
DOI: 10.1016/J.AUTCON.2022.104440

[11] Y. Celik, I. Petri, M. Barati, Blockchain supported BIM data provenance for construction projects, Comput. Ind., vol. 144, 2023, p. 103768
DOI: 10.1016/j.compind.2022.103768

[12] V. R. Gharehbaghi, E. Noroozinejad Farsangi, M. Noori, T. Y. Yang, Sh. Li, A. Nguyen, Ch. Málaga-Chuquitaype, P. Gardoni, S. Mirjalili, A Critical Review on Structural Health Monitoring: Definitions, Methods, and Perspectives, Arch. Comput. Methods Eng., vol. 29, no. 4, 2022, pp. 2209–2235.
DOI: 10.1007/s11831-021-09665-9

[13] A. Sofi, J. Jane Regita, B. Rane, H. H. Lau, Structural health monitoring using wireless smart sensor network – An overview, Mech. Syst. Signal Process., vol. 163, Jan. 2022, p. 108113.
DOI: 10.1016/J.YMSSP.2021.108113

[14] P. Kot, M. Muradov, M. Gkantou, G. S. Kamaris, K. Hashim, D. Yeboah, Recent Advancements in Non-Destructive Testing Techniques for Structural Health Monitoring, Appl. Sci. 2021, Vol. 11, Page 2750, vol. 11, no. 6, Mar. 2021, p. 2750.
DOI: 10.3390/APP11062750

[15] K. Máthé, L. Buşoniu, Vision and Control for UAVs: A Survey of General Methods and of Inexpensive Platforms for Infrastructure Inspection, Sensors 2015, Vol. 15, Pages 14887-14916, vol. 15, no. 7, Jun. 2015, pp. 14887–14916.
DOI: 10.3390/S150714887

[16] R. Rani Hemamalini, R. Vinodhini, B. Shanthini, P. Partheeban, M. Charumathy, K. Cornelius, Air quality monitoring and forecasting using smart drones and recurrent neural network for sustainable development in Chennai city, Sustain. Cities Soc., vol. 85, Oct. 2022, p. 104077.
DOI: 10.1016/J.SCS.2022.104077

[17] D. Choi, W. Bell, D. Kim, J. Kim, UAV-Driven Structural Crack Detection and Location Determination Using Convolutional Neural Networks, Sensors 2021, Vol. 21, Page 2650, vol. 21, no. 8, Apr. 2021, p. 2650.
DOI: 10.3390/S21082650

[18] S. Sankarasrinivasan, E. Balasubramanian, K. Karthik, U. Chandrasekar, R. Gupta, Health Monitoring of Civil Structures with Integrated UAV and Image Processing System, Procedia Comput. Sci., vol. 54, 2015, pp. 508–515.
DOI: 10.1016/j.procs.2015.06.058

[19] B. Han, S. Ding, X. Yu, Intrinsic self-sensing concrete and structures: A review, Measurement, vol. 59, Jan. 2015, pp. 110-128.
DOI: 10.1016/J.MEASUREMENT.2014.09.048

[20] C. Rainieri, G. Fabbrocino, E. Cosenza, Integrated seismic early warning and structural health monitoring of critical civil infrastructures in seismically prone areas, vol. 10, no. 3, Jun. 2010, pp. 291–308.
DOI: 10.1177/1475921710373296

[21] D. D. L. Chung, Electrically conductive cement-based materials, vol. 16, no. 4, May 2015, pp. 167–176.
DOI: 10.1680/adcr.2004.16.4.167

[22] C. G. Berrocal, K. Hornbostel, M. R. Geiker, I. Löfgren, K. Lundgren, D. G. Bekas, Electrical resistivity measurements in steel fibre reinforced cementitious materials, Cem. Concr. Compos., vol. 89, May 2018, pp. 216–229.
DOI: 10.1016/j.cemconcomp.2018.03.015

[23] B. G. Han, B. Z. Han, X. Yu, B. G. Han, B. Z. Han, X. Yu, Experimental study on the contribution of the quantum tunneling effect to the improvement of the conductivity and piezoresistivity of a nickel powder-filled cement-based composite, SMaS, vol. 18, no. 6, 2009, p. 065007.
DOI: 10.1088/0964-1726/18/6/065007

[24] M. S. Konsta-Gdoutos and C. A. Aza, Self sensing carbon nanotube (CNT) and nanofiber (CNF) cementitious composites for real time damage assessment in smart structures, Cem. Concr. Compos., vol. 53, 2014, pp. 162–169.
DOI: 10.1016/j.cemconcomp.2014.07.003

[25] Y. Suo, H. Xia, R. Guo, Y. Yang, Study on self-sensing capabilities of smart cements filled with graphene oxide under dynamic cyclic loading, J. Build. Eng., vol. 58, Oct. 2022, p. 104775.
DOI: 10.1016/J.JOBE.2022.104775

[26] M. Chen, P. Gao, F. Geng, L. Zhang, H. Liu, Mechanical and smart properties of carbon fiber and graphite conductive concrete for internal damage monitoring of structure, Constr. Build. Mater., vol. 142, 2017, pp. 320–327.
DOI: 10.1016/j.conbuildmat.2017.03.048

[27] A. Mobili, A. Belli, Ch. Giosuè, M. Pierpaoli, L. Bastianelli, A. Mazzoli, M. L. Ruello, T. Bellezze, F. Tittarelli, Mechanical, durability, depolluting and electrical properties of multifunctional mortars prepared with commercial or waste carbon-based fillers, Constr. Build. Mater., vol. 283, 2021, p. 122768.
DOI: 10.1016/j.conbuildmat.2021.122768

[28] A. O. Monteiro, P. B. Cachim, P. M. F. J. Costa, Self-sensing piezoresistive cement composite loaded with carbon black particles, Cem. Concr. Compos., vol. 81, 2017, pp. 59–65.
DOI: 10.1016/j.cemconcomp.2017.04.009

[29] A. Mobili, G. Cosoli, N. Giulietti, P. Chiariotti, G. Pandarese, T. Bellezze, G. M. Revel, F. Tittarelli, Effect of Gasification Char and Recycled Carbon Fibres on the Electrical Impedance of Concrete Exposed to Accelerated Degradation, Sustainability, vol. 14, 2022,

no. 3, p. 1775.
DOI: 10.3390/su14031775

[30] G. Lacanna, M. Ripepe, M. Coli, R. Genco, E. Marchetti, Full structural dynamic response from ambient vibration of Giotto's bell tower in Firenze (Italy), using modal analysis and seismic interferometry, NDT E Int., vol. 102, Mar. 2019, pp. 9–15.
DOI: 10.1016/J.NDTEINT.2018.11.002

[31] S. Elias, R. Rupakhety, D. De Domenico, S. Olafsson, Seismic response control of bridges with nonlinear tuned vibration absorbers, Structures, vol. 34, Dec. 2021, pp. 262–274.
DOI: 10.1016/J.ISTRUC.2021.07.066

[32] S. Oliveira, A. Alegre, Seismic and Structural Health Monitoring of Dams in Portugal, 2019, pp. 87–113.
DOI: 10.1007/978-3-030-13976-6_4

[33] F. Wenner, A method for measuring Earth resistivity, J. Washingt. Acad. Sci., vol. 5, no. 16, 1915, pp. 561–563.

[34] O. Galao, F. J. Baeza, E. Zornoza, P. Garcés, Strain and damage sensing properties on multifunctional cement composites with CNF admixture, Cem. Concr. Compos., vol. 46, 2014, pp. 90–98.
DOI: 10.1016/j.cemconcomp.2013.11.009

[35] G. Cosoli, A. Mobili, N. Giulietti, P. Chiariotti, G. Pandarese, F. Tittarelli, T. Bellezze, N. Mikanovic, G. M. Revel, Performance of concretes manufactured with newly developed low-clinker cements exposed to water and chlorides: Characterization by means of electrical impedance measurements, Constr. Build. Mater., vol. 271, 2021, p. 121546.
DOI: 10.1016/j.conbuildmat.2020.121546

[36] F. Tittarelli, A. Mobili, P. Chiariotti, G. Cosoli, N. Giulietti, A. Belli, G. Pandarese, T. Bellezze, G. M. Revel, Cement-Based Composites in Structural Health Monitoring, ACI Symp. Publ., vol. 355, 2022, pp. 133–150.

[37] M. Collepardi, The new concrete, 2010. Online [Accessed 31 January 2022]
https://www.libreriauniversitaria.it/new-concrete-collepardi-mario-tintoretto/libro/9788890377723

[38] A. Mobili, G. Cosoli, T. Bellezze, G. M. Revel, F. Tittarelli, Use of gasification char and recycled carbon fibres for sustainable and durable low-resistivity cement-based composites, J. Build. Eng., vol. 50, 2022, p. 104237.
DOI: 10.1016/j.jobe.2022.104237

[39] M. Mastali, A. Dalvand, A. Sattarifard, The impact resistance and mechanical properties of the reinforced self-compacting concrete incorporating recycled CFRP fiber with different lengths and dosages, Compos. Part B, vol. 112, 2017, pp. 74-92.
DOI: 10.1016/j.compositesb.2016.12.029

[40] S. Takemura, M. Kobayashi, K. Yoshimoto, Prediction of maximum P- and S-wave amplitude distributions incorporating frequency- and distance-dependent characteristics of the observed apparent radiation patterns 4. Seismology, Earth, Planets Sp., vol. 68, no. 1, Dec. 2016, pp. 1–9.
DOI: 10.1186/S40623-016-0544-8

[41] P. Tosi, P. Sbarra, V. De Rubeis, Earthquake sound perception, Geophys. Res. Lett., vol. 39, no. 24, p. 24301.
DOI: 10.1029/2012GL054382